

Uncertainty management in peer-to-peer energy trading based on blockchain and distributed model predictive control ^{*}

Manuel Sivianes ^{*} Pablo Velarde ^{**} Ascensión Zafra-Cabeza ^{*}
José M. Maestre ^{*} Carlos Bordons ^{****}

^{*} *Systems Engineering and Automation Department, University of Seville, Spain (e-mails: {mscastano, asunzafra, pepemaestre}@us.es).*

^{**} *Departamento de Ingeniería, Universidad Loyola Andalucía, Spain. (e-mail: pavelarde@uloyola.es).*

^{****} *ENGREEN Laboratory of Engineering for Energy and Environmental Sustainability, University of Seville, Spain. (e-mail: bordons@us.es).*

Abstract: This work presents a distributed energy management platform based on a smart contract displayed on a blockchain network to optimize the behavior of an energy community under stochastic disturbances, such as solar irradiance and agents' energy demands. Disturbances are modeled as probability distributions and are handled by a distributed model predictive control scheme based on chance constraints. The performance of the proposed algorithm is assessed across various simulations.

Copyright © 2023 The Authors. This is an open access article under the CC BY-NC-ND license (<https://creativecommons.org/licenses/by-nc-nd/4.0/>)

Keywords: energy and distribution management systems, blockchain, stochastic control, predictive control.

1. INTRODUCTION

Microgrids offer various advantages, including reducing costs, increasing efficiency, and providing stability in managing the challenges posed by renewable energy sources to meet electricity demand and reduce carbon footprints. These networks can work in conjunction with the utility grid or in an island mode using storage systems (García-Torres et al., 2021). The control problem in microgrids aims to meet energy demand despite uncertainties in energy generation, electricity market prices, and unanticipated electricity requests. Numerous works have been developed to address this problem using various control techniques. Review papers, such as (Minchala-Avila et al., 2015), provide an overview of these techniques, and (Zafra-Cabeza et al., 2020) provides a centralized controlled microgrid overview, including risk analysis using hierarchical control.

In this context, Model Predictive Control (MPC) is an optimal control strategy suitable for dealing with nonlinearities, process delays, and constraints on variable systems (Camacho and Bordons, 2013). MPC strategy involves solving an optimization problem to minimize a specific objective function over a prediction horizon (N_h), subject to a discrete-time linear model that predicts the future behavior of the system and constraints on both inputs

and outputs to guide the system toward a reference point. The optimization problem is built and solved at each time instant, with the first element applied to the system using a receding horizon strategy.

Energy management systems must consider uncertainties when dealing with demand and renewable generation (Bordons et al., 2020). The standard formulation of an MPC controller does not consider these sources of uncertainty. Several alternatives to classical MPC have been developed to address non-deterministic behavior in power systems operation, see. e.g., (Velarde et al., 2017), and references therein.

In this sense, Chance-Constrained MPC (CC-MPC) is suitable for dealing with uncertainties. In this case, constraints are tightened according to a certain risk level considering the probability distribution of the uncertainties, which can be approximated based on historical data. For example, CC-MPC has been used successfully in some power systems, see e.g., (Vergara-Dietrich et al., 2019; Márquez et al., 2021).

In geographically distributed systems like the power grid, centralized MPC approaches are not directly applicable due to the presence of multiple decision-makers and the need for redundancy (Maestre and Negenborn, 2013). An example of a distributed system is an EC, which consists of a network of end users designed to provide economic, social, and environmental benefits to its members while meeting the energy demand of the entire system. In these situations, local MPC controllers, also called agents, govern the subsystems composing the whole system. This approach, known as Distributed MPC (DMPC), possesses

^{*} This work has received funding from the European Research Council (ERC) under the European Union's Horizon 2020 research and innovation program (OCONTSOLAR, grant agreement No 789051), project C3PO-R2D2 (Grant PID2020119476RB-I00 funded by MCIN/AEI/ 10.13039/501100011033), and Grant PID2019-104149RB-I00 funded by MCIN/AEI/ 10.13039/501100011033.

the necessary modularity for this application and reduces the computation burden compared to centralized MPC. However, coordinating multiple controllers requires a significant exchange of information to achieve optimality, either hierarchically or in a distributed manner, which can lead to security or privacy breaches (Maestre et al., 2021).

This need for security can be addressed by handling blockchain technology, which can provide security by enabling trustworthy peer-to-peer transactions and removing intermediaries (Nakamoto, 2008). Distributed Ledger Technology ensures data integrity by sharing data simultaneously among every node in the network (Nofer et al., 2017). Consensus is reached through algorithms like Proof of Work, Proof of Stake, or Proof of Authority, among others (Yaga et al., 2019). Data are contained in immutable transactions within blocks that are cryptographically linked, making it difficult for malicious agents to take control of the network (Nofer et al., 2017). Furthermore, smart contracts are an important feature of the blockchain ecosystem that allows users to code programs to act according to immutable, user-defined rules. In the context of microgrids or EC with distributed agents participating in distributed optimization algorithms, the smart contract can act as a coordinator, eliminating the need for external companies. Several works, such as (Mengelkamp et al., 2018; van Leeuwen et al., 2020), have used blockchain technology for energy management within microgrids.

The contribution of this work is to extend (Sivianes et al., 2022) in such a way that disturbances are now handled using a stochastic approach. In particular, a DMPC scheme is used to operate an EC composed of various agents affected by uncertainty in both the generation of renewable energy and electricity demand by using blockchain technology. Therefore, the novelty of this work is the proposal of a new approach based on distributed CC-MPC controllers that deal with uncertainty in energy trading systems.

The rest of this paper is organized as follows. Section 2 introduces the problem formulation of energy trading in an EC. The CC-MPC approach is formulated in Section 3, and the negotiation procedure for distributed coupled variables is detailed in Section 4. Section 5 discusses the blockchain implementation, and the results are presented in Section 6. Finally, some conclusions and future directions are drawn in Section 7.

2. PROBLEM FORMULATION

This section describes the equations that model the EC and the performance index to be optimized over the prediction horizon.

2.1 Energy community formulation

The EC consists of two groups of agents: prosumers have access to Distributed Energy Resources (DERs) such as batteries, solar panels, or Evs, while consumers need to import energy from external sources to meet their energy demands. The EC is represented by a complete digraph $\mathcal{G} = (\mathcal{A}, \mathcal{V})$, where $\mathcal{A} = \{1, \dots, n\}$ is the set of agents and $\mathcal{V} \subseteq \mathcal{N} \times \mathcal{N}$ is the set of directed edges between every agent $(i, j) \in \mathcal{A}$. All agents are able to import power from

the UG, denoted by $p^{ug}i, t$, and the excess power sold back to the UG is represented by $p^{ugb}i, t$ and rewarded with a cost of κ_t^b [€/kWh]. The import of $p_{i,t}^{ug}$ incurs a unitary economic cost of κ_t [€/kWh].

Two uncertainty sources are considered within the model: the global horizontal irradiance $\varpi_{i,t}$ [W/m²] and the load demand $p_{i,t}^{ul} \forall i \in \mathcal{A}$. Since the EC is assumed to enclose a relatively small geographical area compared with the variation of $\varpi_{i,t}$ as a function position, $\varpi_{i,t}$ is supposed to be the same $\forall i \in \mathcal{A}$ at each time t , i.e., $\varpi_{i,t} \cong \varpi_t$.

Batteries not only store energy that can be later used, but also handle both energy trading and excess power management. Energy stored in batteries of agent i , is represented by $e_{i,t}^b$ and is computed and constrained as:

$$e_{i,t}^b = e_{i,t-1}^b + (\eta_c^b p_{i,t}^{bc} - \frac{p_{i,t}^{bd}}{\eta_d^b} - \sum_{j \neq i}^n \frac{p_{ij,t}^{bt}}{\eta_t^b}) \Delta t + (\eta^{pv} a_i \varpi_t) \Delta t - p_{i,t}^{ugb} \Delta t, \quad \forall i, t, \quad (1)$$

$$e_{i,t}^b |l \leq e_{i,t}^b \leq e_{i,t}^b |u, \quad \forall i, t, \quad (2)$$

$$0 \leq p_{i,t}^{bc} \leq p_{i,t}^{bc} |u, \quad \forall i, t, \quad (3)$$

$$0 \leq p_{i,t}^{bd} \leq p_{i,t}^{bd} |u, \quad \forall i, t, \quad (4)$$

$$0 \leq p_{ij,t}^{bt} \leq p_{ij,t}^{bt} |u, \quad \forall i, j, t. \quad (5)$$

where $p_{i,t}^{bc}$, $p_{i,t}^{bd}$ and $p_{ij,t}^{bt}$ stand for charging, discharging, and trading power, respectively. The efficiencies of the battery for charging, discharging, and trading are represented by η^{bc} , η^{bd} , and η^{bt} , respectively. The solar panel conversion efficiency and PV area installed are represented by η^{pv} and a_i , respectively. Lower and upper boundaries are denoted by $|l$ and $|u$. The power fed from the battery to meet local demand is denoted by $p^{bd}i, t$, while the power sent from agent i to the EC is represented by $\sum_{j \neq i}^n p_{ij,t}^{bt}$ in equation (1).

Evs are included as flexible loads in which both the time and the demanding charging power, $p_{i,t}^{ev}$, can be controlled. Energy stored within EVs is denoted by $e_{i,t}^{ev}$ and it is calculated as:

$$e_{i,t}^{ev} = e_{i,t-1}^{ev} + \eta_c^{ev} p_{i,t}^{ev} \Delta t, \quad \forall i, t, \quad (6)$$

$$e_{i,t}^{ev} |l \leq e_{i,t}^{ev} \leq e_{i,t}^{ev} |u, \quad \forall i, t, \quad (7)$$

$$0 \leq p_{i,t}^{ev} \leq v_{i,t} p_i^{ev} |u, \quad \forall i, t, \quad (8)$$

where η_c^{ev} is the EV charging efficiency. v is a binary parameter that represents the Ev charging availability, i.e., each agent has a predefined timetable $\Upsilon_i = [v_{1,i}, \dots, v_{\text{end},i}]$ that indicates the time steps at which the Ev will be at the agent's charging point location. An EV daily energy charge of e_{daily}^{ev} is required to satisfy and it is implemented as follows:

$$e_{i,t}^{ev} = e_{i,\text{daily}}^{ev} \quad \forall i \in \mathcal{E}, t = t^{ev} \quad (9)$$

where \mathcal{E} is the set of agents equipped with an EV, and t^{ev} is the time at which EVs must have received the required e_{daily}^{ev} . Here, $p_{i,t}^{ug}$ is computed as the difference between demand and delivered energy as a result of the power balance, i.e.,

$$p_{i,t}^{ug} = p_{i,t}^{bc} - p_{i,t}^{bd} - \sum_{j \neq i}^n p_{ji,t}^{bt} + p_{i,t}^{ul} + p_{i,t}^{ev} \quad \forall i, t, \quad (10)$$

$$p_{i,t}^{ug} \geq 0, \quad \forall i, t, \quad (11)$$

in which $\sum_{j \neq i}^n p_{j,i,t}^{\text{bt}}$ corresponds to the power sent from the EC to agent i .

Finally, these equations can be expressed in a discrete linear time-invariant system as follows:

$$x_{t+1} = A \cdot x_t + B \cdot u_t + D \cdot \omega_t, \quad (12)$$

where $x_t = [\hat{p}_t^{\text{ug}}, \hat{e}_t^{\text{ev}}, \hat{e}_t^{\text{b}}]^T$, $u_t = [\hat{p}_t^{\text{bc}}, \hat{p}_t^{\text{bd}}, \hat{p}_t^{\text{bt}}, \hat{p}_t^{\text{ugb}}, \hat{p}_t^{\text{ev}}]^T$, and $\omega_t = [\hat{\omega}_t, \hat{p}_t^{\text{ul}}]^T$ denote the states, inputs, and disturbances of the system, respectively; accent $\hat{\cdot}$ aggregates a state, input or disturbance for all agents. Matrices A , B , and D include the corresponding coefficients of equations (1), (6), and (11).

To simplify future allusions, closed polyedra \mathcal{X} from state constraints (2),(7),(11), and \mathcal{U} from input constraints (3)-(5),(8),(9), are defined. The constraints can be written as

$$x_{t+1} \in \mathcal{X}, \quad (13a)$$

$$u_t \in \mathcal{U}. \quad (13b)$$

2.2 Performance index

The performance index Φ to be minimized aims to find a trade-off among the economic cost derived from the purchase of p^{ug} , the control effort, and the reference tracking of e^{b} as follows:

$$\begin{aligned} \Phi = & \sum_{t=1}^{N_h} (c_t \hat{p}_t^{\text{ug}} + \delta^{\text{b}}(e_t^{\text{b}}|u - \hat{e}_t^{\text{b}}) + \delta^{\text{ev}}(e_t^{\text{ev}}|u - \hat{e}_t^{\text{ev}})) \\ & + c_{N_h+1} \hat{p}_{N_h+1}^{\text{ug}} + \delta^{\text{b}}(e_{N_h+1}^{\text{b}}|u - \hat{e}_{N_h+1}^{\text{b}}) \\ & + \delta^{\text{ev}}(e_{N_h+1}^{\text{ev}}|u - \hat{e}_{N_h+1}^{\text{ev}}) + \sum_{t=1}^{N_h} u_t^T R u_t, \quad (14) \end{aligned}$$

where R is a matrix of proper dimensions that penalizes p^{bc} , p^{bd} , and p^{bt} . Likewise, it incentivizes p^{ugb} with a weight factor $-\gamma c_t$, with $\gamma < 1$. Note that, since $\gamma < 1$, prosumers will always try to mitigate a neighbor's power deficit before selling power to the UG through p^{ugb} at a $100(1 - \gamma \%)$ discount.

3. STOCHASTIC MPC FORMULATION

CC-MPC approach combines the benefits of MPC with probabilistic constraints to address uncertainties in energy systems. In CC-MPC, uncertain constraints can be converted into deterministic ones by assuming a risk of violation, and the nominal objective function is replaced by its expected value ($\mathbb{E}[\Phi]$).

3.1 Standard MPC Formulation

MPC strategy consists of solving an optimization problem at each time step, t , to compute a set of manipulated variables along N_h . Only the first component, u_t , is applied at the current time, while the remaining elements are discarded. The optimization problem is formulated as

$$\arg \min_{u[t:t+N_h-1]} \Phi, \quad (15)$$

subject to (12) and (13).

The optimization problem (15) is repeated at the next time step, $t + 1$, in a receding horizon fashion.

3.2 CC-MPC Formulation

The uncertainties in solar radiation and energy demand in the load affect the state e^{b}, t , which represents the energy stored in the batteries, as described in equation (1). It should be noted that p^{ul}, t indirectly affects e^{b}, t by replacing $p_{i,t}^{\text{bc}}$ from equation (10) in equation (1). Thus, equation (2) can be converted into a chance constraint where the constraint is satisfied with a specified probability by using the risk of violating the constraint, δ_x , i.e.,

$$\mathbb{P} [e_i^{\text{b}}|l \leq e_{i,t}^{\text{b}} \leq e_i^{\text{b}}|u] \geq 1 - \delta_x. \quad (16)$$

Here, $\mathbb{P}[\cdot]$ is the probability operator. The stochastic variables considered, i.e., $\eta^{\text{pv}} a_i \varpi_t \Delta t$ and $p_{i,t}^{\text{ul}} \Delta t$, are modeled as known cumulative distribution functions (cdf). The deterministic equivalent of the chance constraint is formulated as

$$\begin{aligned} \mathbb{P} [e_{i,t}^{\text{b}} \geq e_i^{\text{b}}|l] \geq 1 - \delta_x & \Leftrightarrow \mathbb{P} [e_{i,t}^{\text{b}} < e_i^{\text{b}}|l] \leq \delta_x \Leftrightarrow \\ \phi_i (e_i^{\text{b}}|l - e_{i,t}^{\text{b}}) \leq \delta_x & \Leftrightarrow e_i^{\text{b}}|l - e_{i,t}^{\text{b}} \leq \phi_i^{-1}(\delta_x) \Leftrightarrow \\ e_{i,t}^{\text{b}} & \geq e_i^{\text{b}}|l + \phi_i^{-1}(1 - \delta_x). \quad (17) \end{aligned}$$

Here, ϕ is the corresponding cdf of the random variable for each agent along N_h . It can be obtained from a known stochastic cdf or based on historical data. An equivalent deterministic chance constraint for the upper limit can be derived in a similar manner, as

$$e_{i,t}^{\text{b}} \leq e_i^{\text{b}}|u - \phi_i^{-1}(1 - \delta_x). \quad (18)$$

Furthermore, the stochastic variable has been modeled as normal distribution functions with a mean and standard value of μ and σ , respectively, that is, $\phi_i = \mathcal{N}(\mu_i, \sigma_i^2)$.

To this end, the optimization problem to be solved by the CC-MPC controller can be expressed as

$$\arg \min_{u[t:t+N_h-1]} \mathbb{E}[\Phi], \quad (19)$$

subject to (7), (11), (12), (13b), (17), and (18).

4. DISTRIBUTED MPC

To solve the CC-MPC in a distributed way, the Feasible Cooperation-Based MPC (FC-MPC) algorithm of Venkat et al. (2005) is used to solve the CC-MPC formulation. The main idea behind this approach is to set $\forall i \in \mathcal{A}$, a cost function that measures the performance of the entire system, e.g., a convex combination of every local cost function Φ_i :

$$\Phi = \sum_{i=1}^n \alpha_i \Phi_i, \quad (20)$$

with $\alpha_i > 0$ and $\sum_{i=1}^n \alpha_i = 1$. The FC-MPC algorithm guarantees plant-wide feasibility of the intermediate iterates, meaning that even if the computation time is higher than the time required for convergence, the control sequence computed during the last iteration is plant-wide feasible. The DMPC formulation is computed $\forall i \in \mathcal{A}$ for a number of iterations p :

$$U_i^* \in \arg(\text{FC-MPC}_i), \quad \text{where} \quad (21)$$

$$\text{FC-MPC}_i \triangleq \min_{u_i} \frac{1}{N} \Phi_i,$$

subject to

$$x_i(t+1) = A \cdot x_i(t) + B \cdot u_i(t) + D \cdot w(t),$$

$$\forall t \in \{1, \dots, N_h\}, \quad (22)$$

and (13), $\forall t \in \{1, \dots, N_h + 1\}$.

The optimized control sequence for each agent i is stored in U_i^* , and the state and input variables are denoted by x_i and u_i . The model optimizes only the variables belonging to each agent, while the rest remain as constant values from the previous iteration.

The stages to solve the FC-MPC algorithm are shown in Algorithm 1, where superscript p refers to the p -th iteration. The goal is to get every agent to compute a pair of control and state sequences $(x_i^p; U_i^p)$ that differ less than the admissible error μ from those computed in the previous iteration. The error between two consecutive iterations of the agent i is defined as ϑ_i^p . As mentioned above, each agent solves (21) taking into account the information provided by his neighbors during the previous iteration and gets U_i^* . Then, $x_i^{p,*}$ is obtained after substituting $U_i^{p,*}$, and $U_{j \neq i}^{p,*}$ in (22). Ultimately, $(x_i^p; U_i^p)$ are determined as a linear combination of $(x_i^{p-1}, x_i^{p,*}; U_i^{p-1}, U_i^{p,*})$, and ϑ_i^p is computed. If $\forall \vartheta_i^p \leq \varkappa$, termination is reached.

Algorithm 1 FC-MPC algorithm

Given $u_i^0, x^0, c_t \geq 0, p^{\max} > 0, \varkappa > 0, p \leftarrow 1, \forall \vartheta_i^1 \gg 1, \phi_i, i \in \mathcal{A}$

while $\vartheta_i^p > \varkappa$ for some $i \in \mathcal{A}$ and $p \leq p_{max}$ **do**

for $i \in \mathcal{A}$ **do**

$U_i^{p,*} \in \arg(\text{FC-MPC}_i, \text{eq. (21)})$

end for

for $i \in \mathcal{A}$ **do**

$x_i^{p,*} \leftarrow x_i^{(u_i^{p,*}, u_{j \neq i}^{p,*}, x^0)}$ in eq. (22)

$(x_i^p, u_i^p) = \frac{1}{N}(x_i^{p,*}, u_i^{p,*}) + (1 - \frac{1}{N})(x_i^{p-1}, u_i^{p-1})$

$\vartheta_i^p = \|(x_i^p, u_i^p) - (x_i^{p-1}, u_i^{p-1})\|$

end for

$p \leftarrow p + 1$

end while

5. BLOCKCHAIN IMPLEMENTATION

One of the main concerns discussed in this work is to address a distributed optimization problem without relying on a centralized coordinator who has complete control and freedom over the algorithm. A smart contract deployed within a blockchain can replace a centralized coordinator in a distributed optimization problem. Ethereum blockchain (Buterin et al., 2013), a public and permissionless blockchain, enables the creation of Turing complete smart contracts through Solidity¹, which is an object-oriented, high-level programming language designed to target the Ethereum Virtual Machine². The smart contract functions as a replacement for the coordinator, performing information exchange between agents, data storage, and distributed algorithm control flow. Note that a smart contract is immutable once it is deployed within the blockchain. This means that no changes can be made to the contract's code or state, making it easier to audit the process.

¹ <https://docs.soliditylang.org/en/develop/index.html>

² <https://ethereum.org/en/developers/docs/evm/>

Next, the software tools used to implement the blockchain are described. The Ethereum testnet Rinkeby³ is used for development and testing. A graphic user interface is developed using React⁴, and web3.js, which enables agents to interact with the smart contract. Web3.js⁵ is a set of libraries that allows users to link to an Ethereum node, and Infura⁶, which provides the Ethereum node. MetaMask serves as the Ethereum wallet. A simplified diagram displaying the interconnection between these tools can be seen in Figure 1.

Algorithm 2 incorporates a smart contract into the distributed optimization problem. The main differences from Algorithm 1 are that agents must upload the current state and a feasible initial control sequence to the smart contract before the first iteration, and during the iterations, agents need to interact with the smart contract to upload $u_i^{p,*}$ and retrieve $u_j^{p,*}, \forall j \in \mathcal{A} - i$. The smart contract also evaluates the terminating condition.

Algorithm 2 Blockchain-based FC-MPC algorithm

Given $c_t \geq 0, p^{\max} > 0, \varkappa > 0, p \leftarrow 1, \forall \vartheta_i^1 \gg 1, \phi_i, i \in \mathcal{A}$

while $\vartheta_i^p > \varkappa$ for some $i \in \mathcal{A}$ and $p \leq p_{max}$ **do**

if $p = 1$ **then**

for $i \in \mathcal{A}$ **do**

 • Compute FC-MPC _{i} with $p_{i,j,t}^b|_{u=0}$.

 • Upload $u_i^{1,*}$ and x_i^1 to the smart contract.

 • Retrieve $u_j^{1,*}$ and $x_j^1 \forall j \in \mathcal{A} - i$ from the smart contract.

end for

 Smart contract:

for $i \in \mathcal{A}$ **do**

 • Collect $u_i^{1,*}$ and x_i^1 .

end for

 • Assemble global $U^{1,*}$ and x^1 matrices.

else

for $i \in \mathcal{A}$ **do**

 • Compute FC-MPC _{i} .

 • Upload $u_i^{p,*}$ to the smart contract.

 • Retrieve $u_j^{p,*} \forall j \in \mathcal{A} - i$ from the smart contract.

 • Calculate:

$x_i^{p,*} \leftarrow x_i^{(u_i^{p,*}, u_{j \neq i}^{p,*}, x^1)}$ in eq. (22)

$(x_i^p, u_i^p) = \frac{1}{N}(x_i^{p,*}, u_i^{p,*}) + (1 - \frac{1}{N})(x_i^{p-1}, u_i^{p-1})$

$\vartheta_i^p = \|(x_i^p, u_i^p) - (x_i^{p-1}, u_i^{p-1})\|$

 • Upload ϑ_i^p to the smart contract.

end for

 Smart contract:

for $i \in \mathcal{A}$ **do**

 • Collect ϑ_i^p .

end for

 • Check the terminating condition.

 • $p = p + 1$.

end if

end while

6. RESULTS AND DISCUSSION

This section presents a case study to evaluate the performance of the distributed Algorithm 2. Different simulation settings are considered, and the results are compared and evaluated.

³ <https://ethereum.org/en/developers/docs/networks/>

⁴ <https://es.reactjs.org/>

⁵ <https://web3js.readthedocs.io/en/v1.3.4/>

⁶ <https://docs.infura.io/infura/>

6.1 Case study

The EC consists of 15 agents with 7 prosumers and 8 consumers. Prosumers have a battery, solar panels, and an EV, while consumers can only buy power from the UG or via power trades. The cost of buying power from the grid is based on the clearing prices of the Iberian Electricity Market, and the selling price of p_t^{ugb} back to the grid is $c_t^{ugb} = 0.5c_t, \forall t$. The simulations start at midnight in September and for $N_h = 24$ hours, it covers a full day.

Solar radiation and power demand are treated as normal distribution functions. For the load, data were obtained from (Palacios-Garcia et al., 2018) to generate the agent's hourly consumption profiles for a year. Here, these data are used to generate bimonthly normal distributions for each hour as, on the one hand, a yearly data set is divided into $M = 6$ groups of 2 consecutive months each. On the other

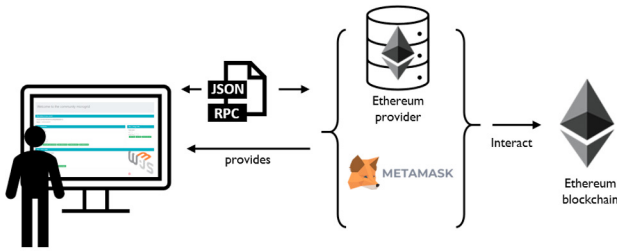


Fig. 1. Interconnection between the distributed application elements.

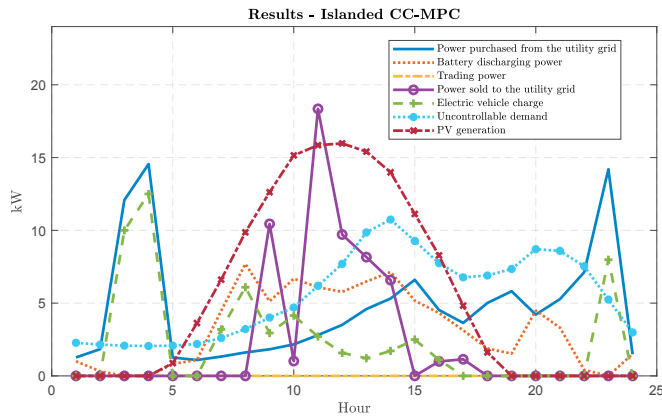


Fig. 2. Results isolated test.

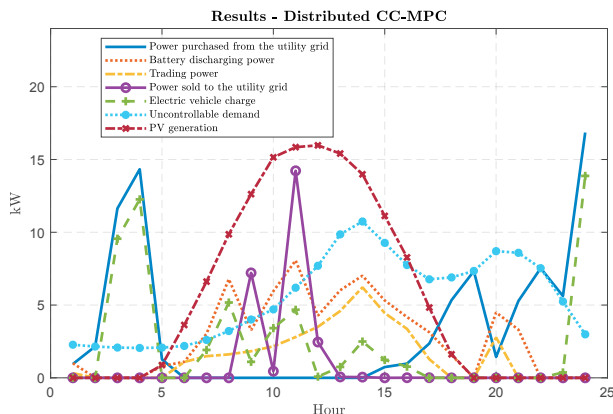


Fig. 3. Results CC-DMPC test.

hand, for each subset, defined as $\Omega_m^{p^{ul}}, \forall m \in \{1, \dots, M\}$, an equivalent normal distribution function is generated $\phi_{i,t,m}^{p^{ul}} = \mathcal{N}(\mu_i^{\Omega_m^{p^{ul}}}, \sigma_i^{\Omega_m^{p^{ul}}}), \forall t \in \{1, \dots, 24\}$.

The exact same process is repeated for solar radiation, where data are gathered from PVGIS Photovoltaic Geographical Information System⁷, leading to $\phi_{i,t,m}^{\sigma} = \mathcal{N}(\mu_i^{\Omega_m^{\sigma}}, \sigma_i^{\Omega_m^{\sigma}}) \forall t \in \{1, \dots, 24\}$.

The prosumers are equipped with a single battery with an energy capacity ranging from 3.3 to 3.9 kWh, and charging, discharging, and trading efficiencies of 94.5%, 94.5%, and 93%, respectively. The lower and upper bounds for the battery's energy level are set as $e_i^b|_l=28\%$ and $e_i^b|_u=87\%$ of the maximum energy capacity. For EVs, the daily energy charge is between 7.25 and 8.35 kWh, with a charging time of 24 hours. The EV availability timetable is generated randomly and the upper limit of power for EV charging is set at 2.5 kW. The charging efficiency of EV is 0.95.

6.2 Simulations

Simulations were carried out in three test scenarios to compare the proposed control strategies. The first scenario was an islanded approach where power trades between agents were not allowed. The second scenario was the distributed CC-MPC (CC-DMPC) approach, where power trades were enabled, and a risk of constraint violation was set at 5%. The third scenario was the standard DMPC, which did not consider the stochastic nature of disturbances. The results of the simulations for each scenario are shown in Figures 2, 3, and 4, respectively.

Results are shown in Table 1, where both economic and performance indexes are defined as E_1 : economic cost of purchasing power from the UG, E_2 : profit of selling power to the UG, E_3 : difference between E_1 and E_2 , E_4 : energy exchanged between agents, E_5 : energy sold back to the UG, E_6 : energy purchased from the UG, E_7 : energy purchased from the UG by consumers, and E_8 : energy purchased from the UG by prosumers.

⁷ https://joint-research-centre.ec.europa.eu/pvgis-photovoltaic-geographical-information-system_en

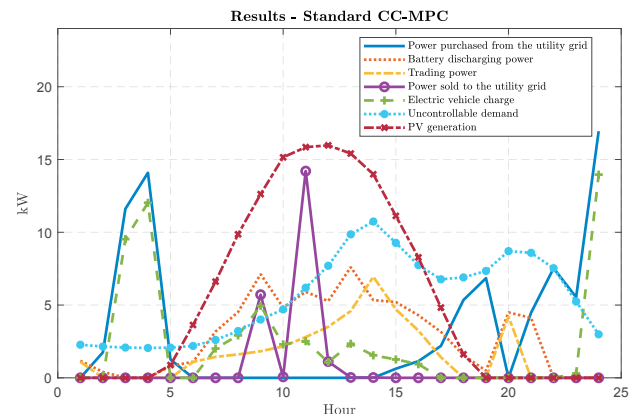


Fig. 4. Results standard DMPC test.

Table 1. Simulation results

Indexes	Tests		
	Islanded CC-MPC	Distributed CC-MPC	Standard MPC
E_1 [€]	38.59	28.86	27.09
E_2 [€]	11.68	5.25	4.57
E_3 [€]	26.90	23.61	22.52
E_4 [kWh]	0	37.49	40.66
E_5 [kWh]	56.40	24.47	21.15
E_6 [kWh]	113.13	83.80	79.35
E_7 [kWh]	59.37	30.04	27.71
E_8 [kWh]	53.76	53.76	51.64

6.3 Performance assessment

Considering the economic and performance indexes shown in Table 1, the lowest E_1 is found in the Islanded CC-MPC test since power trades are not enabled and prosumers cannot help consumers reduce their consumption p^{ug} .

The results show that CC-DMPC and standard DMPC have a lower dependence on the microgrid than Islanded CC-MPC, reducing E_1 . Islanded CC-MPC has higher values for E_2 and E_5 due to excess solar power generation. Standard MPC has the lowest value for E_3 , while CC-DMPC and standard DMPC reduce the gap between $e_i^p|u$ and $e_i^b|l$, leading to less battery usage in terms of power trading, reflected in E_4 . In E_7 and E_8 , it is shown that consumers' consumption is slightly higher than prosumers' in Islanded CC-MPC, but this changes drastically when power trades are enabled. Finally, E_8 remains constant in both Islanded CC-MPC and CC-DMPC tests due to the surplus of energy from solar generation, allowing prosumers to obtain a greater global benefit from the consumer side without assuming any performance loss.

7. CONCLUSIONS AND FUTURE WORK

This study has presented the energy management in an EC affected by uncertainty in both solar irradiance and energy demand. The stochastic nature of the disturbances has been addressed by using a CC-MPC controller in each agent of the system. Moreover, the DMPC scheme is based on a smart contract deployed in Rinkeby and serves as a global coordinator of the distributed algorithm without relying on a central authority. The results show that CC-MPC and blockchain algorithms, jointly working, are suitable for carrying out a negotiation process among agents to satisfy the energy demand despite uncertainties. Future work will focus on new EC formulations and secure DMPC schemes to enhance the obtained results.

REFERENCES

- Bordons, C., Garcia-Torres, F., and Ridao, M.A. (2020). *Model predictive control of microgrids*. Springer.
- Buterin, V. et al. (2013). Ethereum white paper. *GitHub repository*, 1, 22–23.
- Camacho, E.F. and Bordons, C. (2013). *Model predictive control*. Springer science & business media.
- Garcia-Torres, F., Zafra-Cabeza, A., Silva, C., Grieu, S., Darure, T., and Estanqueiro, A. (2021). Model predictive control for microgrid functionalities: Review and future challenges. *Energies*, 14(5), 1296.
- Maestre, J.M. and Negenborn, R.R. (2013). *Distributed MPC Made Easy*. Intelligent Systems, Control and Automation: Science and Engineering. Springer-Verlag, Vol. 69, New York, USA.
- Maestre, J.M., Velarde, P., Ishii, H., and Negenborn, R.R. (2021). Scenario-based defense mechanism against vulnerabilities in lagrange-based dmcp. *Control Engineering Practice*, 114, 104879.
- Mengelkamp, E., Gärttner, J., Rock, K., Kessler, S., Orsini, L., and Weinhardt, C. (2018). Designing microgrid energy markets: A case study: The brooklyn microgrid. *Applied Energy*, 210, 870–880.
- Minchala-Avila, L.I., Garza-Castañón, L.E., Vargas-Martínez, A., and Zhang, Y. (2015). A review of optimal control techniques applied to the energy management and control of microgrids. *Procedia Computer Science*, 52, 780–787.
- Márquez, J., Zafra-Cabeza, A., Bordons, C., and Ridao, M.A. (2021). A fault detection and reconfiguration approach for MPC-based energy management in an experimental microgrid. *Control Engineering Practice*, 107, 104695.
- Nakamoto, S. (2008). Bitcoin: A peer-to-peer electronic cash system. *Decentralized Business Review*, 21260.
- Nofer, M., Gomber, P., Hinz, O., and Schiereck, D. (2017). Blockchain. *Business & Information Systems Engineering*, 59(3), 183–187.
- Palacios-Garcia, E., Moreno-Munoz, A., Santiago, I., Flores-Arias, J., Bellido-Outeirino, F., and Moreno-Garcia, I. (2018). A stochastic modelling and simulation approach to heating and cooling electricity consumption in the residential sector. *Energy*, 144, 1080–1091.
- Sivianes, M., Zafra-Cabeza, A., and Bordons, C. (2022). Blockchain-based peer to peer energy trading using distributed model predictive control. In *Proceedings of the 2022 European Control Conference (ECC)*, 1832–1837. IEEE, London, United Kingdom.
- van Leeuwen, G., AlSkaif, T., Gibescu, M., and van Sark, W. (2020). An integrated blockchain-based energy management platform with bilateral trading for microgrid communities. *Applied Energy*, 263, 114613.
- Velarde, P., Valverde, L., Maestre, J.M., Ocampo-Martínez, C., and Bordons, C. (2017). On the comparison of stochastic model predictive control strategies applied to a hydrogen-based microgrid. *Journal of Power Sources*, 343, 161–173.
- Venkat, A.N., Rawlings, J.B., and Wright, S.J. (2005). Stability and optimality of distributed model predictive control. In *Proceedings of the 44th IEEE Conference on Decision and Control*, 6680–6685. Seville, Spain.
- Vergara-Dietrich, J.D., Morato, M.M., Mendes, P.R., Cani, A.A., Normey-Rico, J.E., and Bordons, C. (2019). Advanced chance-constrained predictive control for the efficient energy management of renewable power systems. *Journal of Process Control*, 74, 120–132.
- Yaga, D., Mell, P., Roby, N., and Scarfone, K. (2019). Blockchain technology overview. *arXiv preprint arXiv:1906.11078*.
- Zafra-Cabeza, A., Velarde, P., and Maestre, J.M. (2020). Multicriteria optimal operation of a microgrid considering risk analysis, renewable resources, and model predictive control. *Optimal Control Applications and Methods*, 41(1), 94–106.